Novel Morphologies of Block Copolymer Blends via Hydrogen Bonding

Shimei Jiang,† Astrid Göpfert, and Volker Abetz*

Makromolekulare Chemie II, Universität Bayreuth, D-95440 Bayreuth, Germany

Received March 7, 2003; Revised Manuscript Received May 20, 2003

ABSTRACT: A polystyrene-*block*-poly(1,2-butadiene)-*block*-poly(*tert*-butyl methacrylate) (SBT) triblock copolymer and its analogues with different degrees of saponification, SB(T/A) with A being poly(methacrylic acid) are characterized in terms of their morphologies and infrared spectroscopic features. The chemical modification of the third block leads to a change of the overall morphology from a gyroid to a lamellar structure. Blends of these SB(T/A) triblock copolymers with polystyrene-*block*-poly(2-vinylpyridine) (SV) diblock copolymer and poly(2-vinylpyridine)-*block*-poly(cyclohexyl methacrylate) (VC) diblock copolymer were prepared and characterized. Attractive segmental interactions through hydrogen bonds between A and V blocks have been monitored by infrared spectroscopy. Upon increasing the amount of proton donors, the amount of hydrogen bonds between A and V units also increased. Superlattices composed of the two block copolymers were obtained by casting films from a mixed solution of these block copolymers in tetrahydrofuran (THF) and were investigated by transmission electron microscopy (TEM). Varying the amount of hydrogen-bonding donors via controlled saponification of the SBT triblock copolymer lead to different superlattices in blends with SV and VC diblock copolymers.

Introduction

In recent years, considerable progress has been made in recognizing the importance of specific interactions in the phase behavior of polymer blends. One of the most important intermolecular interactions is the hydrogen bond between a proton donor and a proton acceptor. The hydrogen bond can be responsible for the miscibility of otherwise incompatible polymers, as well as enhancing the miscibility of partially miscible systems.[1−9]

Furthermore, attractive enthalpic interactions can lead to miscibility of different blocks. Although attractive interactions between some blocks of a block copolymer and other homopolymers or random copolymers have been used to compatibilize the interesting blends,[10−12] this strategy has never been used by other groups to generate common superlattices of different block copolymers. The concept of using hydrogen bonds to create a higher level of hierarchy in structure formation was used by Ikkalas' group in blends of a diblock copolymer and low molecular chains, which were bound to one of the blocks via hydrogen bonds.[13] In a previous contribution, first results on blends of different block copolymers were presented, where hydrogen bonding was used as an attractive enthalpic interaction between different block copolymers.[14] In particular blends of SB(T/A) triblock copolymers with SV or VC diblock copolymers were presented (S, polystyrene; B, poly(1,2-butadiene); T, poly(*tert*-butyl methacrylate); A, poly(methacrylic acid); V, poly(2-vinylpyridine); C, poly(cyclohexyl methacrylate)), where attractive enthalpic interactions can be expected between A and V end blocks. The results presented in that paper demonstrated the possibility to generate superlattices in block copolymer blends by using specific attractive interactions of different blocks. However, blends of SV or VC with SBA did not show a long range ordered morphology. One reason for this might be the very strong interactions between the A and V blocks. A reduction of the strength of these acid−base interactions could be reached by reducing the number of interacting groups. In fact, blending SV with SB(T/A) containing a reduced number of hydrogen-bond-forming groups lead to well-orderered superlattices. Another problem in such blends is the poor solubility of the poly(methacrylic acid) in THF which is due to the strong hydrogen bonds between the A units. Thus, it is likely that the A units microphase separate first from solution, while S and B blocks are still soluble in it. One way to solve this problem might be to use triblock copolymers which contain less A units.

In this contribution, we will consider controlling the amount of hydrogen-bonding donor units. Poly(*tert*-butyl methacrylate) (T) can be saponified to poly(methacrylic acid)(A). Through controlling the degree of saponification of the SBT triblock copolymer we may get a series of SB(T*m*/A*n*) triblock copolymers containing different amounts of proton donor units (A). Then we use this series of SB(T*m*/A*n*) triblock copolymers to prepare blends with SV or VC diblock copolymers. In these blends via employing SB(T*m*/A*n*) triblock copolymers containing less A (with respect to the pure SBA), first we may reduce the possibility of phase separation during film formation as the solvent is evaporating as was pointed out before,[15] and second we could decrease the strong interactions between A and V units via "diluting" the A units with large amount of T units. Finally we will see how the hydrogen-bonding strength has a dramatic effect on the different block copolymer blends.

Experimental Part

Synthesis of Block Copolymers. Polystyrene-*block*-poly(2-vinylpyridine) ($S_{45}V_{55}^{76}$) diblock copolymer, poly(2-vinylpyridine)-*block*-poly(cyclohexyl methacrylate) ($V_{58}C_{42}^{59}$) diblock copolymer, and polystyrene-*block*-poly(1,2-butadiene)-*block*-poly(*tert*-butyl methacrylate) ($S_{17}B_{53}T_{30}^{112}$) triblock copolymer were synthesized by sequential anionic polymerization of the different monomers. The details of the synthesis have been described elsewhere.[14] The characterization of the polymers is given in Table 1.

* Corresponding author. E-mail: volker.abetz@uni-bayreuth.de.
† Permanent address: Key Laboratory for Supramolecular Structures and Materials, College of Chemistry, Jilin University, Changchun 130023, P. R. China.

10.1021/ma0342933 CCC: $25.00
Published on Web 07/19/2003

Table 1. Characterization of Block Copolymers

block copolymer[a]	M_w(g/mol)	PDI[b]	morphology
$S_{45}V_{55}{}^{76}$	76 000	1.06	lamellae
$V_{58}C_{42}{}^{59}$	29 000	1.05	lamellae
$S_{17}B_{53}T_{30}{}^{112}$	112 100	1.02	double gyroid

[a] Subscripts denote the weight fractions of the corresponding block in percent and the superscript gives the number-averaged molecular weight in kilograms per mole. [b] GPC (THF, PS standards).

Hydrolysis of Triblock Copolymer SBT. $S_{17}B_{53}T_{30}{}^{112}$ was dissolved in a mixture of dioxane and an excess of concentrated aqueous HCl (with respect to the *tert*-butyl groups) and stirred at 95 °C. At different reaction times, some amount of product which contained different degrees of saponification of the *tert*-butyl groups was taken out. The products were precipitated immediately into water. The precipitates were further washed with water until pH = 7.

Fourier Transform Infrared Spectroscopy (FTIR). Infrared spectra were recorded on a Bruker Equinox 55/S FTIR spectrometer at a resolution of 4 cm^{-1}. A total of 128 scans was averaged in all cases. Samples for infrared analysis were prepared by casting thin films on NaCl plates from THF solution. After most of the solvent had evaporated, the sample was placed in a vacuum oven overnight to remove residual solvent. All the films employed in this study are thin enough to obey the Beer−Lambert law.

Transmission Electron Microscopy (TEM). The blend components were dissolved together in THF which was evaporated over several weeks. After that, the cast films were dried under vacuum for 2 days at room temperature, followed by careful increase of temperature to an annealing temperature at 120 °C. For further equilibration, the samples were held at this temperature for 6 h before cooling to room temperature. All of the blend films are optically transparent.

Ultrathin sections of the samples were obtained using a Reichert-Jung Ultracut E equipped with a diamond knife. For samples with a large amount of polybutadiene the ultrathin films were obtained under cryogenic conditions. Staining was achieved by treating the ultrathin section for 40 min with RuO_4 vapor (dark S domains) or for 1 min with OsO_4 vapor (dark B domains)[16] and then for 24 h with CH_3I vapor (gray V domains),[17,18] as indicated in the corresponding figure captions. Electron micrographs were taken from a Zeiss 902 transmission electron microscope operating at 80 kV in the bright-field mode.

Results and Discussion

Modification of SBT Triblock Copolymers. To obtain the proton donor, i.e., SBA triblock copolymer, we modify the SBT triblock copolymer by hydrolysis. In the hydrolysis reaction of SBT, the degree of hydrolysis depends on the amount of HCl and the reaction time. Normally for this kind of hydrolysis the amount of HCl is excessive with respect to the *tert*-butyl group. For a molar ratio of HCl/T-units = 3, after 25 h only 10% T had been converted to A. For a molar ratio of HCl/T-units = 12, after 1 h 90% T had been converted to A. To exactly control the degree of saponification we used a molar ratio of HCl/T-units = 6 for the hydrolysis.

During this hydrolysis, the poly(*tert*-butyl methacrylate) (T) can be saponified to poly(methacrylic acid) (A). That is to say, the *tert*-butyl group will disappear and the carbonyl group will change to a carboxyl group. Fourier transform infrared (FTIR) spectroscopy is very sensitive to the changes of these functional groups. So FTIR spectroscopy was used to follow the hydrolysis reaction by monitoring the change of carbonyl group and the disappearance of the characteristic double bands of the *tert*-butyl group at 1394 and 1367 cm^{-1}.[19]

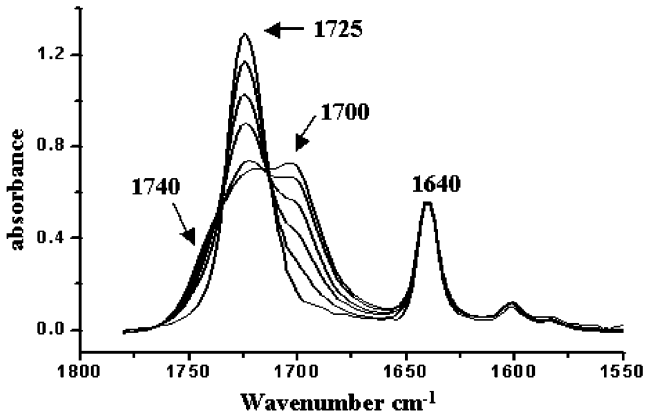

Figure 1. FT-IR spectra of SBT and its analogues with different degrees of saponification, SB(T*m*/A*n*). For the peaks at 1725 cm^{-1} they are SBT, SB(T85/A15), SB(T70/A30), SB(T55/A45), SB(T36/A64), and SB(T30/A70) from top to bottom. For the peaks at 1700 cm^{-1} they have the inverse order.

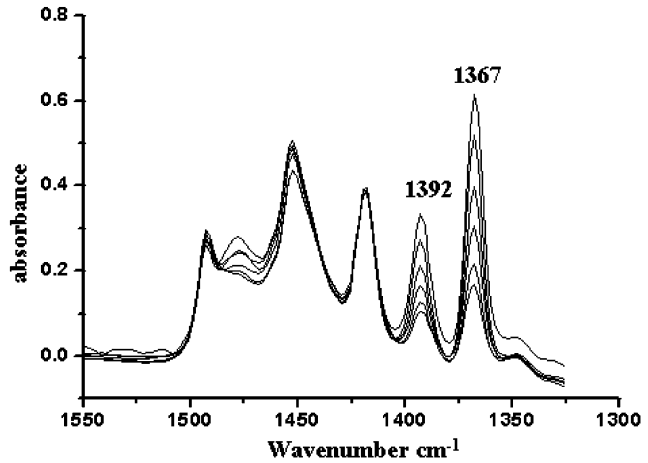

Figure 2. FT-IR spectra of SBT and its analogues with different degrees of saponification, SB(T*m*/A*n*). For the peaks at 1367 and 1392 cm^{-1}, they are SBT, SB(T85/A15), SB(T70/A30), SB(T55/A45), SB(T36/A64), and SB(T30/A70) from top to bottom.

First let us pay attention to the carbonyl stretching region. Figure 1 shows the FTIR spectra of SBT and its analogues SB(T*m*/A*n*) saponified to different degrees in the region 1550−1800 cm^{-1}. For the pure $S_{17}B_{53}T_{30}{}^{112}$ triblock copolymer, 1725 cm^{-1} is assigned to the carbonyl group. As the reaction progressed, the intensity of the 1725 cm^{-1} band decreased. At the same time two new bands corresponding to poly(methacrylic acid) gradually appeared, as shown in Figure 1. One band is located at 1740 cm^{-1} and belongs to the free carboxyl group, and another one is located at 1700 cm^{-1} and belongs to the dimer of methacrylic acid units. This means that during the hydrolysis process, some of the poly(*tert*-butyl methacrylate) units gradually convert to poly(methacrylic acid) units.

Let us now turn our attention to the bands at 1392 and 1367 cm^{-1} which are the characteristic bands of the *tert*-butyl group. Figure 2 shows the intensity changes of these two bands corresponding to different saponification degrees. As the reaction progressed, the intensities of these two bands gradually decreased. When the hydrolysis finished, i.e., SBT triblock copolymers completely converted to SBA, these two characteristic bands will have disappeared.

From the investigations above, all two spectral regions are suitable for quantitative analysis. But the

Table 2. Different Modification Degrees of SBT Triblock Copolymers

	reaction time (min)	A_{1367}/A_{1640}	relative amount of T blocks (%)	triblock copolymer[b]	morphology
SBT		0.9218	100	$S_{17}B_{53}T_{30}^{112}$	double gyroid
SB(T88/A12)[a]	90	0.8127	88	$S_{17.2}B_{53.8}(T_{26.8}/A_{2.2})^{110.41}$	double gyroid
SB(T82/A18)	120	0.7584	82	$S_{17.4}B_{54.1}(T_{25.2}/A_{3.3})^{109.62}$	double gyroid/lamellae
SB(T75/A25)	150	0.6953	75	$S_{17.5}B_{54.6}(T_{23.2}/A_{4.7})^{108.69}$	double gyroid/lamellae
SB(T64/A36)	240	0.5874	64	$S_{17.8}B_{55.4}(T_{20}/A_{6.8})^{107.23}$	lamellae
SB(T49/A51)	320	0.4510	49	$S_{18.1}B_{56.4}(T_{15.6}/A_{9.9})^{105.24}$	lamellae

[a] SB(T*m*/A*n*): *m* and *n* denote the molar fraction radio of the T and A blocks [b] Subscripts denote the weight fractions of the corresponding block in percent, and the superscript gives the number-averaged molecular weight in kilograms per mole.

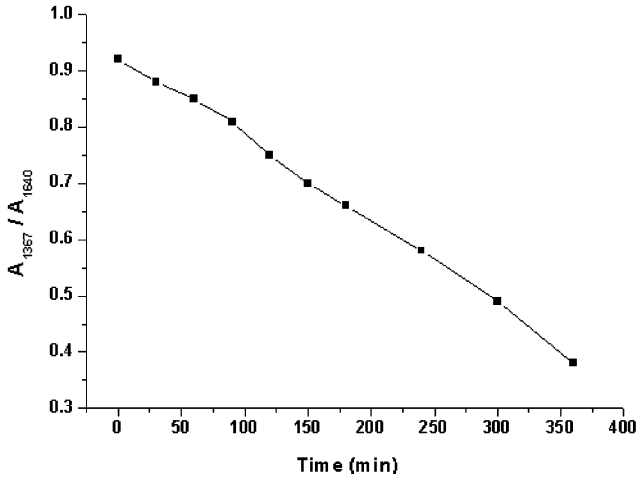

Figure 3. Graph of relative intensities of A_{1367}/A_{1640} vs hydrolysis time.

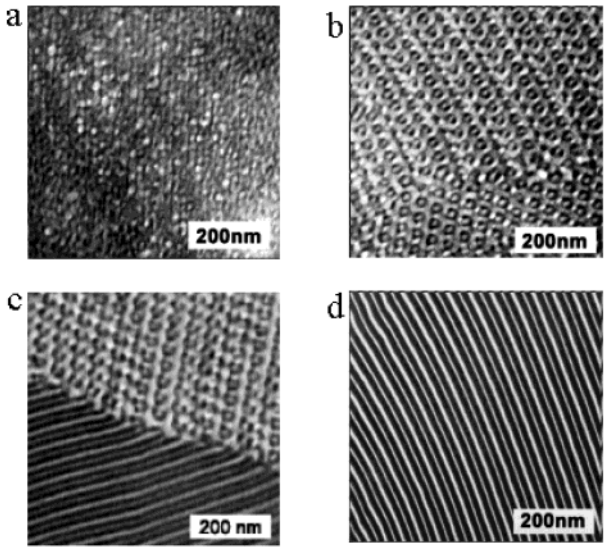

Figure 4. TEM micrographs of SB(T*m*/A*n*) triblock copolymers stained with OsO_4. (a) SBT, (b) SB(T88/A12), (c) SB(T82/A18), and (d) SB(T64/A36).

latter is particularly convenient, because the peaks in the carbonyl group region are overlapped. So we follow the degree of the saponification reaction by monitoring the disappearance of the characteristic double bands of the *tert*-butyl group at 1394 and 1367 cm^{-1}.

The band at 1640 cm^{-1} is assigned to the C=C stretching vibration of poly(1,2-butadiene) (B), as shown in Figure 1. During the saponification this band remains unchanged, so we chose this band as the internal standard to calculate the degree of saponification. The integral areas of the relative bands were used. Figure 3 gives the quantitative analysis based on the 1367 cm^{-1} band. It is obvious that the relative intensities of A_{1367}/A_{1640} linearly decreased as the reaction progressed. This result means that the T units gradually convert to A units with time. So the value of A_{1367}/A_{1640} is proportional to the amount of T units. If we assume the amount of T units for $S_{17}B_{53}T_{30}^{112}$ to be 100%, then we can easily calculate the relative amount of T units for its saponified analogues. The characterization of the modified block copolymers and the details of the saponification are summarized in Table 2. In the case of its different degree of saponified analogues, SB(T*m*/A*n*), *m* and *n* denote the molar fraction in percent of the T and A units, respectively.

The Influences of Modification on the Morphologies of the Series SB(T*m*/A*n*). The aim of controlling the saponificaton of SBT is to obtain a series of SB(T*m*/A*n*) which contain different amounts of hydrogen-bonding donor. First, let us see the influence of this saponification on the morphology of SBT. The pure $S_{17}B_{53}T_{30}^{112}$ triblock copolymer exhibits a double gyroid structure, as shown in Figure 4a. As we increase the degree of saponification to 12%, i.e., SB(T88/A12), again a double gyroid is obtained, as shown in Figure 4b. For conversion ratios about 18% or larger, i.e., SB(T82/A18), besides the double gyroid domains also lamellar domains coexist, as shown in Figure 4c. SB(T75/A25) shows the same morphology. Finally, when the conversion ratio is about 36% or larger, i.e., SB(T64/A36), only lamellae are formed, as shown in Figure 4d. SB(T49/A51) shows the similar lamellar morphology.

FTIR Spectroscopic Studies of the Hydrogen Bonding. Infrared spectroscopy has been proven as a powerful tool for investigating specific interactions between polymers and the mechanism of interpolymer miscibility through the formation of hydrogen bonding.[20−22] Before discussing the morphology of these blends, we will first use FTIR spectroscopy to prove the existence of the attractive interactions between A and V units.

The most striking feature of SB(T*m*/A*n*) blending with SV, however, is the presence of two bands at 2525 and 1946 cm^{-1}, as shown in Figure 5. These are indicative of strong hydrogen bonds between carboxylic acid and pyridine groups.[20,23]

On the other hand, infrared studies show that carboxyl and pyridine ring peaks undergo important changes which are attributed to hydrogen bonding between the carboxyl groups and the nitrogen atom present within the pyridine ring. Figure 6 shows the FTIR spectra of SB(T49/A51), $S_{45}V_{55}$,[76] and the 50 wt %/50 wt % blend of SB(T49/A51) with $S_{45}V_{55}$[76], in the region 1800−1550 cm^{-1}.

First let us pay attention to the carbonyl region. For the spectrum of SB(T49/A51), as we have discussed above, the peak at 1725 cm^{-1} belongs to the carbonyl stretching vibration of the ester group of the residual *tert*-butyl methacrylate units, the bands at 1740 and 1700 cm^{-1} correspond to the free carboxyl group and

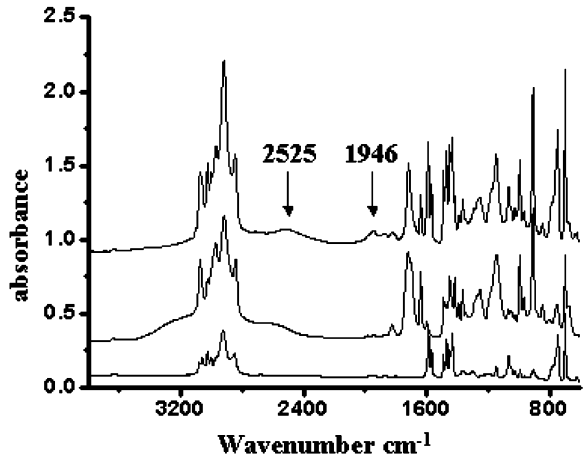

Figure 5. FTIR spectra of $S_{45}V_{55}^{76}$ (bottom), SB(T49/A51) (middle), and the blend of 50 wt % SB(T49/A51) with 50 wt % $S_{45}V_{55}^{76}$ (top).

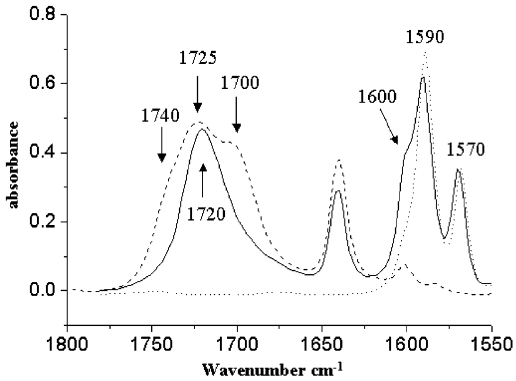

Figure 6. FTIR spectra of SB(T49/A51) (dash), $S_{45}V_{55}^{76}$ (dot), and the blend of 50 wt % SB(T49/A51) with 50 wt % $S_{45}V_{55}^{76}$ (solid).

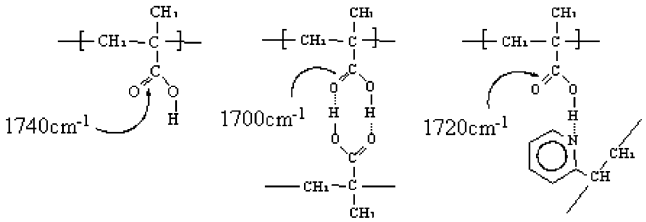

Figure 7. Assignment of the different vibrations in SBA and SBA/SV blend.

the dimer of methacrylic acid units, respectively (Figure 6, dashed line).

Let us consider the spectrum of the blend (Figure 6, solid line). In the carbonyl stretching region the two bands corresponding to methacrylic acid units (1740 and 1700 cm^{-1}) disappeared. A new band at about 1720 cm^{-1} appears, which is indicative of a complex of a carboxyl group with the pyridine nitrogen atom, as shown in Figure 7. Next we inspect the influences on the proton acceptors. In the spectrum of $S_{45}V_{55}^{76}$ (Figure 6, dotted line), the absorption of pyridine group is located at 1590 and 1570 cm^{-1}. The phenyl group of the styrene units also exhibits a very weak absorption at 1600 cm^{-1}. In the blend spectrum (Figure 6, solid line), the 1570 cm^{-1} band appears insensitive to the formation of the complex. Comparing to this band, the band intensity of 1590 cm^{-1} is decreased. Conversely, the intensity of the 1600 cm^{-1} band is increased. The band at 1600 cm^{-1} is characteristic of the pyridine-carboxylic acid interaction and results from a perturbation of the 1590 cm^{-1} ring

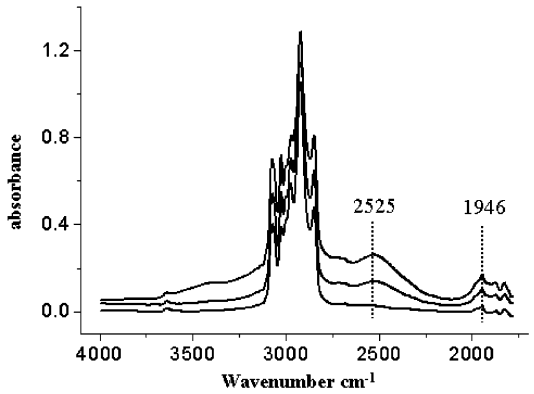

Figure 8. FTIR spectra of SB(T*m*/A*n*) blended with $S_{45}V_{55}^{76}$. From bottom to top: SB(T85/A15), SB(T49/A51), and SB(T15/A85) blended with $S_{45}V_{55}^{76}$.

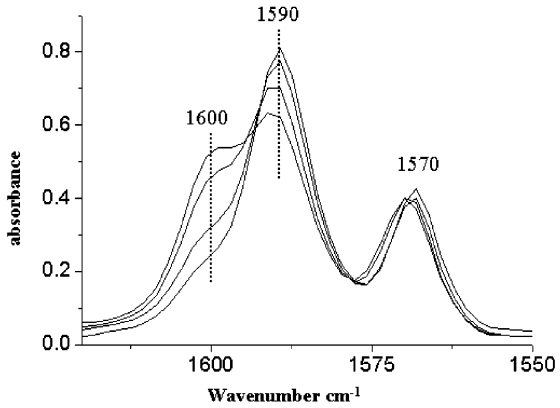

Figure 9. FTIR spectra of $S_{45}V_{55}^{76}$ and SB(T*m*/A*n*) blended with $S_{45}V_{55}^{76}$. For the peaks at 1590 cm^{-1}, they are pure $S_{45}V_{55}^{76}$, SB(T85/A15) blended with $S_{45}V_{55}^{76}$, SB(T49/A51) blended with $S_{45}V_{55}^{76}$, and SB(T15/A85) blended with $S_{45}V_{55}^{76}$ from top to bottom. For the peaks at 1600 cm^{-1}, they have the inverse order.

mode.[22] So the band at 1600 cm^{-1} is an overlap of the phenyl groups and the complexed pyridine groups. As the spectrum of pure $S_{45}V_{55}^{76}$ in this region shows, the absorption arising from phenyl group is small, so this intensity change is mainly attributed to the formation of complex between carboxyl group and pyridine nitrogen.

FTIR Spectroscopic Studies of the Attractive Interactions in the Blends. Through controlling the degree of saponification of the SBT triblock copolymer we get a series of SB(T*m*/A*n*) triblock copolymers containing different amounts of proton donor units (A). We used these SB(T*m*/A*n*) triblock copolymers to prepare the blends with $S_{45}V_{55}^{76}$ diblock copolymer. For all of the blends presented here the weight composition between triblock copolymer and diblock copolymer is 50:50.

By FTIR spectroscopy we have proven that there is hydrogen bonding between the methacrylic acid units (A) and pyridine units (V) in the blends of SB(T/A) with SV. Now we want to investigate the relationship between the number of attractive interactions and the amount of proton donors.

We chose a series of SB(T*m*/A*n*) containing different amount of proton donors, i.e., SB(T85/A15), SB(T49/A51), and SB(T15/A85), to prepare the blends with $S_{45}V_{55}^{76}$. Figures 8−10 show the FTIR spectra of these blends as a function of the amount of proton donors. When we increase the amount of A units from SB(T85/

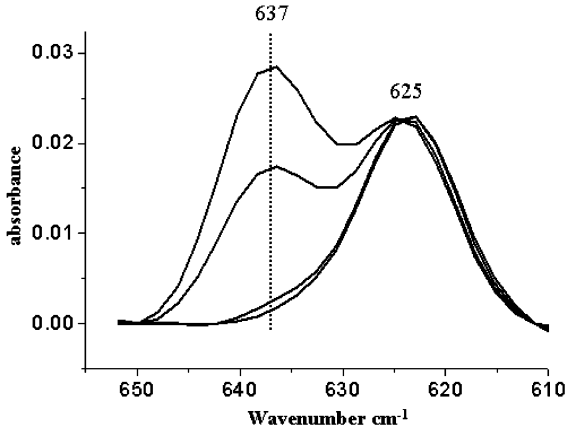

Figure 10. FTIR spectra of $S_{45}V_{55}^{76}$ and SB(T*m*/A*n*) blended with $S_{45}V_{55}^{76}$. From bottom to top: pure $S_{45}V_{55}^{76}$, SB(T85/A15) blended with $S_{45}V_{55}^{76}$, SB(T49/A51) blended with $S_{45}V_{55}^{76}$, and SB(T15/A85) blended with $S_{45}V_{55}^{76}$.

A15) to SB(T15/A85), the intensities of the two characteristic bands (2525 and 1946 cm^{-1}) also increased, as shown in Figure 8. It is obvious that there is strong hydrogen bonding between A and V units. As we increase the amount of proton donors, the number of the hydrogen bonding also increased. Next we inspect the influences of this variation on the proton acceptors. For the $S_{45}V_{55}^{76}$ diblock copolymer the absorptions at 1590 and 625 cm^{-1} correspond to the ring modes of the free pyridine groups.[22] Upon formation of the hydrogen bond with A units, these bands shift to higher frequencies at 1600 and 637 cm^{-1}, respectively, as shown in Figure 9 and Figure 10. This effect is attributed to the changes in the electron distribution in the pyridine ring due to the formation of stronger bonds.[21] In Figure 9, as we have proven above, the 1570 cm^{-1} band appears insensitive to the formation of the complex. We can use this band as an internal standard. From Figure 9, it is obvious that in the blends of SB(T*m*/A*n*) with $S_{45}V_{55}^{76}$ the band intensity at 1590 cm^{-1}, which is attributed to the free pyridine ring, decreased as the amount of proton donors (A units) was increased. Conversely, the band intensity at 1600 cm^{-1} increased. Because we increased the amount of proton donors (A units), they consumed more and more proton acceptors (V units) to form the hydrogen-bonding complexes. So the band intensities corresponding to the free proton acceptors decreased and the band intensities corresponding to the hydrogen-bonding complexes increased. Parallel changes are also observed for the pyridine ring modes at 637/625 cm^{-1}, as shown in Figure 10. As the amount of proton donors (A units) is increased in the blend, there is a corresponding increase in the relative intensity of the 637 cm^{-1} as compared to the band at 625 cm^{-1}. These results show that with increasing the amount of proton donors the amount of hydrogen bonds also increases in these blends.

The Influence of Hydrogen Bonding on the Morphologies of Blends. The blend of SBT with SV is macrophase separated. Then we introduced the proton donor to the triblock copolymer, i.e., we modified T to A units. Because of the hydrogen bonding between A and V units, the formation of an ordered superlattice was expected for the blend of SBA with SV. However, the blend of SBA with SV did not show a long range ordered morphology. So we considered to use partly modified SBT triblock copolymers, i.e., SB(T*m*/A*n*) for the blends. As we have pointed out above, for these blends via employing SB(T*m*/A*n*) triblock copolymers

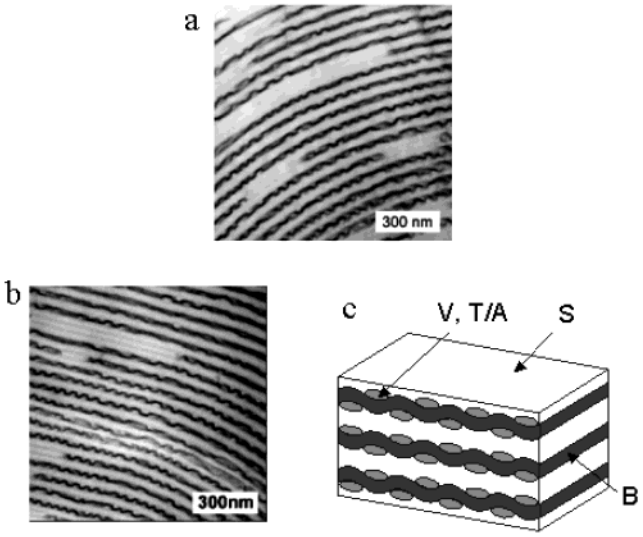

Figure 11. TEM micrographs of SB(T88/A12) blended with $S_{45}V_{55}^{76}$: (a) stained with OsO_4; (b) stained with OsO_4 and CH_3I; (c) arrangement of the different microphases.

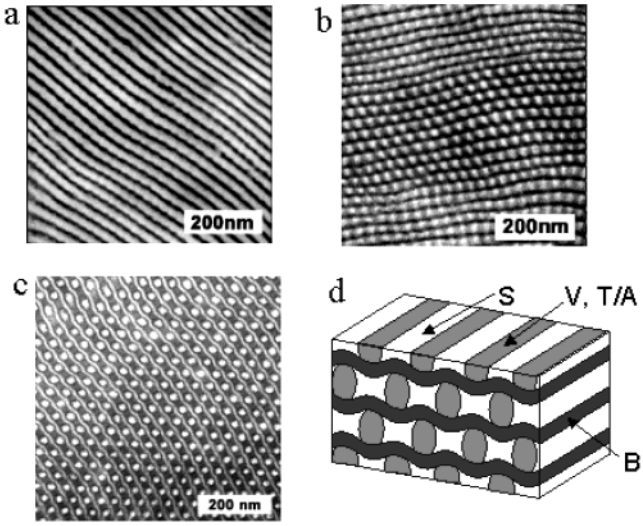

Figure 12. TEM micrographs of SB(T82/A18) blended with $S_{45}V_{55}^{76}$: (a) stained with OsO_4; (b) stained with OsO_4 and CH_3I; (c) stained with RuO_4; (d) the arrangement of the different microphases according to Figure 12, parts a and b.

containing less A (with respect to the pure SBA), first we may reduce the possibility of phase separation due to the poor solubility of A block, second we could decrease the strong interactions between A and V blocks via "diluting" the A units with large amount of T units. In this case, we may expect to obtain long-range ordered superlattices.

The FTIR investigations proved the existence of attractive interactions between triblock copolymers SB(T*m*/A*n*) and diblock copolymer SV. Now let us see how does the hydrogen bond strength influence the morphologies of these blends.

1. Blend of SB(T88/A12) with $S_{45}V_{55}^{76}$. Figure 11 shows the TEM micrographs of SB(T88/A12) blended with $S_{45}V_{55}^{76}$. First we used OsO_4 as the staining agent for the TEM investigation. In this case, only polybutadiene (B) appears black in the TEM micrographs. As shown in Figure 11a, B forms curved domains within lamellae of the other components.

Since OsO_4 can only stain B domains, we chose CH_3I to stain in addition the domains of poly(2-vinylpyridine)

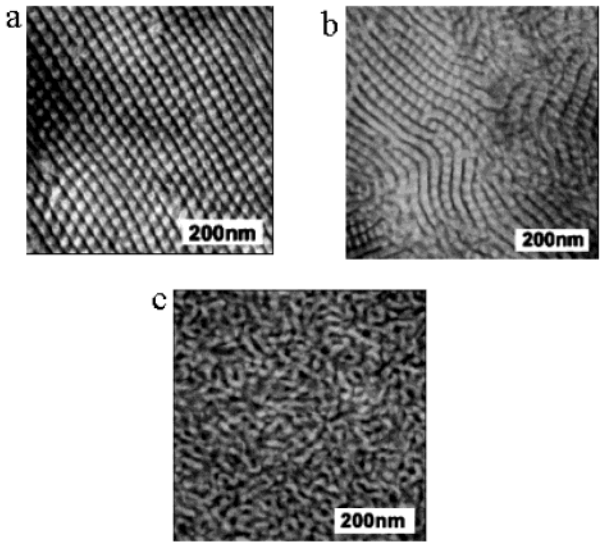

Figure 13. TEM micrographs of SB(T*m*/A*n*) blended with $S_{45}V_{55}^{76}$ stained with OsO_4 and CH_3I: (a) SB(T75/A25); (b) SB(T64/A36); (c) SB(T49/A51) blended with $S_{45}V_{55}^{76}$.

(V).[17] Under this condition the B appears black, V appears gray, S appears slightly gray, and T and A remain unstained.

Figure 11b shows the TEM micrograph of this blend stained with OsO_4 and CH_3I. It is obvious that there are some areas corresponding to pure SV lamellae. Following the traces of V lamellae in the pure SV domains, one can recognize the V domains in the superlattice. As schematically shown in Figure 11c, B forms curved lamellae within the S lamellae, and the T/A···V domains are located on both sides of B. In this case the chain sequence is as follows: SB(T/A)···VSSV···(A/T)BS or V···(A/T)BSSB(T/A)···V.

2. Blend of SB(T82/A18) with $S_{45}V_{55}^{76}$. Figure 12 shows the TEM micrographs of SB(T88/A18) blended with $S_{45}V_{55}^{76}$. Figure 12a shows the micrograph stained with OsO_4. In this case, the B block forms curved lamellar domains. The double staining with OsO_4 and CH_3I shows hexagonally packed cylinders of the other blocks within the curved B lamellae, as shown in Figure 12b. The white domains are formed by mixed S of diblock and triblock copolymer, while the gray domains should be the mixed blocks of V and T/A. To further confirm this morphology we also used RuO_4 as a staining agent. In this case the S block appears black, and the B block is gray, while T, A, and V blocks remain unstained (Figure 12c). Also the interfaces between different components are stained by this agent. Figure 12c confirms the interpretation of Figure 12, parts a and b. A scheme of the morphology according to Figure 12, parts a and b, is given in Figure 12d.

3. Blends of SB(T*m*/A*n*) Containing Higher Amounts of A Units with $S_{45}V_{55}^{76}$. Figure 13 shows the TEM micrographs of SB(T75/A25), SB(T64/A36), and SB(T49/A51) blended with $S_{45}V_{55}^{76}$ and using OsO_4 and CH_3I for staining.

The blends of SB(T75/A25) and SB(T64/A36) with $S_{45}V_{55}^{76}$ show nearly the same morphology as the blend of SB(T88/A18) with $S_{45}V_{55}^{76}$ (Figure 13, parts a and b). However, the order of the morphology seems to be decreased for the systems with more A units, which could indicate a problem with the solubility of the T/A blocks in THF. In line with this argument, the blend of SB(T49/A51) with $S_{45}V_{55}^{76}$ does not form a well-ordered morphology at all (Figure 13c).

Blends of SB(T*m*/A*n*) with $V_{58}C_{42}^{59}$ Block Copolymers. From the above investigations, it is obvious that through hydrogen bonding between triblock copolymer and diblock copolymer we can generate common super-

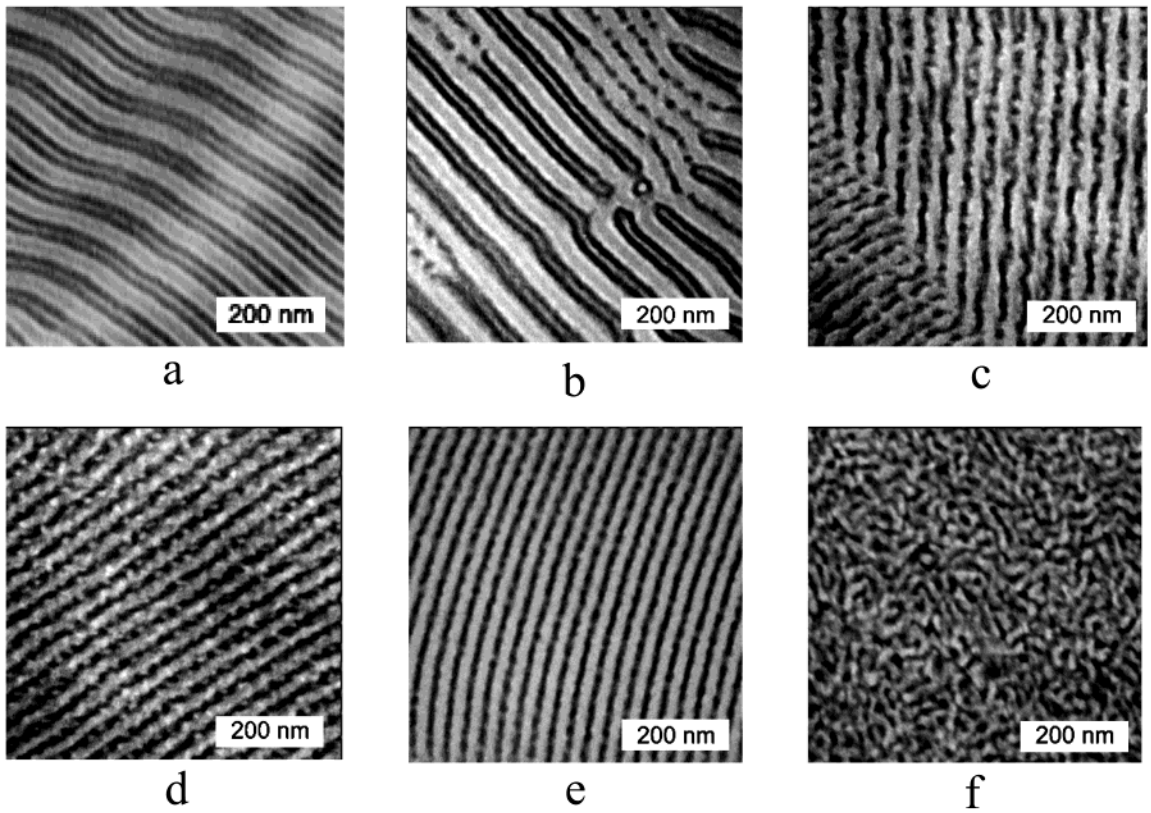

Figure 14. TEM micrographs of SB(T*m*/A*n*) blended with $V_{58}C_{42}^{59}$ stained with OsO_4 and CH_3I: (a) SBT; (b) SB(T88/A12); (c) SB(T82/A18); (d) SB(T75/A25); (e) SB(T64/A36); (f) SB(T49/A51) blended with V58C42 59.

lattices of the two species via self-assembly from their mixed solutions. Now we use another diblock copolymer, which is poly(2-vinylpyridine)-*block*-poly(cyclohexyl methacrylate) ($V_{58}C_{42}^{59}$). In the blends of SB(T*m*/A*n*) with $V_{58}C_{42}^{59}$, apart from the attractive interaction between A and V, also the favorable interaction between polystyrene (S) and poly(cyclohexyl methacrylate) (C) is expected. The miscibility between S and C homopolymers was reported to originate from local packing entropy effects.[24]

Figure 14a shows the blend of $S_{17}B_{53}T_{30}^{112}$ with $V_{58}C_{42}^{59}$. It shows alternating double lamellae of triblock copolymer and diblock copolymer with the chain sequence ···SBTTBS CVVC SBTTBS···. This is nicely seen by the alternating shorter and longer distances between the black B lamellae. As all the morphologies discussed so far, it is centrosymmetric. Note that the same triblock copolymer showed macrophase separation, when being blended with $S_{45}V_{55}$.[76] This means that there was a mismatch of block lengths and stretching energy of the S-blocks of diblock and triblock copolymer preventing them from formation of mixed domains.[25] In the blend with VC, the specific interactions between S and C lead to the formation of a common superlattice, proving the compatibility between these two blocks.

Figure 14b shows the TEM micrograph of SB(T88/A12) blended with $V_{58}C_{42}^{59}$. It shows basically the same morphology as Figure 14a, but due to some hydrogen bonds the B lamellae show defects, thus allowing direct contacts between V and T/A blocks. For SB(T*m*/A*n*) with higher amount of A, as in the cases of SB(T82/A18), SB(T75/A25) and SB(T64/A36), the blends with $V_{58}C_{42}^{59}$ also show mixed domains of T/A and V. Their morphologies change to broken equidistant B lamellae, as shown in Figure 14, parts c−e, respectively. Whether these superlattices are noncentrosymmetric or not cannot be decided clearly. In the case of noncentrosymmetric layering the sequence ···SBT/A VC SBT/A··· should be expected, which would result in equidistant spacings between adjacent B lamellae (compare with the alternating spacings between adjacent B lamellae in the centrosymmetric superlattice in Figure 14a). So far, only a very few examples for self-assembly of block copolymer blends into periodic noncentrosymmetric superlattices were reported.[26−28] Finally, the blend of SB(T49/A51) and $V_{58}C_{42}^{59}$, does not show long range order, as it was found for the corresponding blend of the triblock copolymer with $S_{45}V_{55}^{76}$. This is again attributed to the low solubility of A units in the triblock copolymer.

Conclusion

1. Through controlling the degree of saponification of an SBT triblock copolymer, we get a series of partly modified SB(T*m*/A*n*) triblock copolymers containing different amounts of proton donor units (A). The TEM results show that upon increase of the degree of saponification the morphologies of SB(T*m*/A*n*) block copolymers change from double gyroid to lamellar structure.

2. From the FTIR investigations, it is obvious that there is strong hydrogen bonding between poly(methacrylic acid) (A) units in SB(T*m*/A*n*) triblock copolymer and poly(2-vinylpyridine) units in $S_{45}V_{55}^{76}$ diblock copolymer. When we increase the amount of proton donors via increasing the degree of saponification of SBT triblock copolymer, the amount of hydrogen bonds in the blends also increases.

3. When we blend the pure SBT with $S_{45}V_{55}^{76}$, it macrophase separates. For the blends of SB(T*m*/A*n*) with SV, the introduction of hydrogen bonding between A and V units leads to several superlattices based on the self-assembly of these block copolymers. Their morphologies depend on the amount of the A units. One of them shows hexagonally packed cylinders of (T/A··· V) within curved B lamellae.

4. When blending SB(T*m*/A*n*) with $V_{58}C_{42}^{59}$, apart from the attractive interaction between A and V, S and C also form common microdomains. Some of these blends might form noncentrosymmetric superlattices; however, a more extended study using different block lengths would be necessary to clarify this question.

Acknowledgment. The SBT, VC, and SV block copolymers were synthesized by K. Markgraf. This work was supported by the Deutsche Forschungsgemeinschaft (DFG) through SFB 481.

References and Notes

(1) Rodriguez-Parada, J. M.; Pierce, V. *J. Polym. Sci., Part A: Polym. Chem.* **1986**, *24*, 579.
(2) Isasi, J. R.; Cesteros, L.; Katime, I. *Polymer* **1993**, *24*, 23.
(3) Yoshie, N.; Azuma, Y.; Sakurai, M.; Inoue, Y. *J. Appl. Polym. Sci.* **1995**, *56*, 17.
(4) Lin, L.; Chi-Ming, C.; Lu−Tao, W. *Polymer* **1998**, *39*, 2355.
(5) Etxeberria, A.;, S.; Iruin, J. J.; Campa, J. G.; Abajo, J. *Polymer* **1998**, *39*, 1035.
(6) Rao, V.; Ashokan, P. V.; Shridhar, M. H. *Polymer* **1999**, *40*, 7167.
(7) Cowie, J. M. G.; McEwan, I.; McEwan, I. J.; Pethrick, R. A. *Macromolecules* **2001**, *34*, 7071.
(8) Li, X. D.; Goh, S. H. *J. Polym. Sci., Part B: Polym. Phys.* **2002**, *40*, 1125.
(9) Kou, S. W.; Chang, F. C. *Macromol. Chem. Phys.* **2001**, *16*, 202.
(10) Auschra, C.; Stadler, R. *Macromolecules* **1993**, *26*, 6364.
(11) Cowie, J. M. G.; Love, C. *Polymer* **2001**, *42*, 4783.
(12) Kosonen, H.; Ruokolainen, J.; Torkkeli, M.; Serimaa, R.; Nyholm, P.; Ikkala, O. *Macromol. Chem. Phys.* **2002**, *203*, 388.
(13) Ruokolainen, J.; Makinen, R.; Torkkeli, M.; Makela, T.; Serimaa, R.; Ten Brinke, G.; Ikkala, O. *Science* **1998**, *280*, 557.
(14) Markgraf, K.; Abetz, V. *e-Polym.* **2001**, No. 15.
(15) Abetz, V.; Markgraf, K.; Rebizant, V. *Macromol. Symp.* **2002**, *177*, 139.
(16) Kato, K. *Polym Lett.* **1996**, *4*, 35.
(17) Kunz, M.; Möller, M.; Cantow, H. J. *Makromol. Chem. Rapid Commun.* **1987**, *8*, 401.
(18) Möller, M.; Lenz, R. W. *Makromol. Chem.* **1989**, *190*, 1153.
(19) Bieringer, R.; Abetz, V.; Müller, A. H. E. *Eur. Phys. J. E.* **2001**, *5*, **5.**
(20) Motzer, H. R.; Painter, P. C.; Coleman, M. M. *Macromolecules* **2001**, *34*, 8390.
(21) Cesteros, L. C.; Meaurio, E.; Katime, I. *Macromolecules* **1993**, *26*, 2323.
(22) Lee, J. Y.; Painter, P. C.; Coleman, M. M. *Macromolecules* **1988**, *21*, 954.
(23) Jiang, S. M.; Xu, W. Q.; Zhao, B.; Tian, Y. Q.; Zhao, Y. Y. *Mater. Sci. Eng. C* **2000**, *11*, 85.
(24) Siol, W. *Makromol. Chem., Macromol. Symp.* **1991**, *44*, 47.
(25) Leibler, L.; Gay, C.; Erukhimovich, I. Ya. *Europhys. Lett.* **1999**, *46*, 549.
(26) Goldacker, T.; Abetz, V.; Stadler, R.; Erukhimovich, I.; Leibler, L. *Nature* **1999**, *398*, 137.
(27) Abetz, V.; Goldacker, T. *Macromol. Rapid Commun.* **2000**, *21*, 16.
(28) Abetz, V. Block Copolymers, Ternary Triblocks. In *Encyclopedia of Polymer Science and Technology*, 3rd ed., Kroschwitz, J. I., Ed.; John Wiley & Sons, Inc.: New York, 2003; Vol. 1, pp 482−523.

MA0342933